A Neural Network Modeling of Microwave Circuits on PBG Structures

Everton Notreve Rebouças Queiroz Fernandes [1], Paulo Henrique da Fonseca Silva [2], Adaildo Gomes d'Assunção [3], and Marcos Antonio Barbosa de Melo [4]

[1] Universidade Estadual do Rio Grande do Norte, Mossoró, RN, Brazil, everton.fernandes@terra.com.br
[2] Centro Federal de Educação Tecnológica do Rio Grande do Norte, Mossoró, RN, Brazil
[3] Universidade Federal do Rio Grande do Norte, Caixa Postal 1655, Natal, RN, CEP: 59072-970, Brazil, adaildo@ct.ufrn.br
[4] Universidade Federal de Campina Grande, C. Postal 10053, C. Grande, PB, CEP: 58109-970, Brazil

Abstract — **A new technique is proposed to analyze microwave circuits on uniplanar compact photonic bandgap (UC-PBG) structures. This structure is a two-dimensional square lattice with each element consisting of a metal pad and four connecting branches. The UC-PBG structure can be used in the development of high-performance and compact circuit components for microwave and millimeter-wave frequencies. Usually, accurate analyses of PBG structures are performed through complex techniques, like FDTD. Lately, a growing interest was observed in the use of neurocomputational techniques to study the properties of electromagnetic devices and circuits. The main goal of this work is to develop a new and efficient technique to analyze microwave circuits with UC-PBG based on neural networks. The proposed neural network analysis for UC-PBG structures gave results in excellent agreement with measured results available in the literature. Besides, this technique provided a very good generalization, allowing the comparison with a set of measured results that were not used in the training process.**

I. INTRODUCTION

A PBG structure is a periodic lattice that exhibits a frequency stopband. Therefore, several works have been developed to study the properties of PBG materials for optical band applications. Recently, the use of PBG structures was extended to the development of microwave and millimeter wave circuits [1]-[6].

Lately, a great interest was observed in the study of the uniplanar compact photonic bandgap (UC-PBG) [6]. This structure presents several advantages, including low-loss, broad stopband, and compact size.

There are several microwave applications for UC-PBG structures [5],[6]. For instance, the passband of this structure has been used in the development of slow-wave medium for integrated circuits with reduced dimension [6]. Also, this structure can be used as a magnetic surface at the stopband frequency, to be used in the development of planar reflectors.

UC-PBG structures are also used in rectangular waveguides [6]. These devices are used for applications related to the quasi-optical power coupling.

An accurate analysis of PBG circuits and devices usually requires complex computational techniques, with heavy computational efforts, such as integral equation method [3] and Finite-Difference Time-Domain (FDTD) [6].

Recently, neurocomputational techniques were presented as powerful tools to be used in several applications, including those in microwave engineering [7]. The main characteristics of neural network techniques are generality, adaptability, and generalization ability. Because of that, artificial neural networks (ANNs) techniques are able to properly handle electromagnetic problems such as the analyses of planar transmission lines, waveguide filters, CPW lines, microstrip antennas, FET transistors, and planar spiral inductors [3]-[8].

In this work, the characteristics of microstrip and TEM waveguide photonic bandgap (UC-PBG) structures are investigated. A new neural network paradigm based on the sample function, SFNN, was proposed. The training process was accomplished by using a dataset of measured results available in the literature. It was observed that the outputs of the proposed SFNN technique showed a good agreement with the corresponding measured results for the considered devices.

Besides, the neurocomputational technique showed generalization ability, providing good results for frequencies and structural parameters not considered in the training process.

II. UC-PBG STRUCTURE CHARACTERISTICS

The UC-PBG structure considered in this work is shown in Fig. 1. This structure consists of a periodic two-dimensional lattice printed on a dielectric substrate. The UC-PBG unit cell consists of square pads and narrow lines with insets.

0-7803-7695-1/03/$17.00 © 2003 IEEE

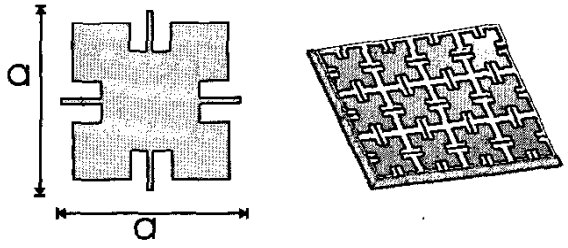

Fig. 1. (a) UC-PBG unit cell. (b) UC-PBG periodic lattice.

The structure shown in Fig. 1 works like a LC distributed circuit with a particular resonant frequency. While the gaps between adjacent unit cells provide the capacitive coupling, the conducting lines provide the inductive coupling, which is increased by insets. At the resonant frequency, corresponding to the stopband frequency of the LC circuit, the periodic load behaves like an open circuit, or an equivalent magnetic surface [8].

The UC-PBG structure is designed according to the resonant frequency, which depends on the introduction of magnetic walls on the periodic element boundary with side dimension **a** (Fig.1).

III. PBG MICROSTRIP LINE DESIGN

Fig. 2 shows a microstrip line on a UC-PBG ground plane.

The UC-PBG section is 720 mil long, which corresponds to six periods. The substrate used is RT/Duroid 6010 with a dielectric constant of 10.2 and dielectric thickness of 25 mil. The microstrip line width is 24 mil, corresponding to a 50-Ω microstrip line with a solid ground plane. A short length of solid ground plane was included at each end of the microstrip line to facilitate the connection with the SMA connectors.

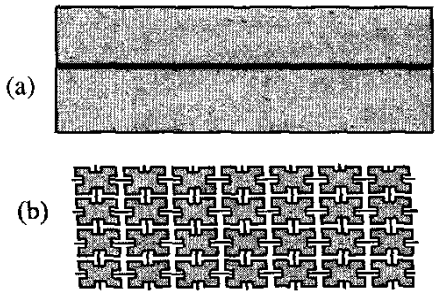

Fig. 2. A microstrip line on a UC-PBG ground plane. (a) Top view. (b) Bottom view.

IV. UC-PBG WAVEGUIDE DESIGN

Fig. 3 shows a TEM rectangular waveguide with two UC-PBG sidewalls [8].

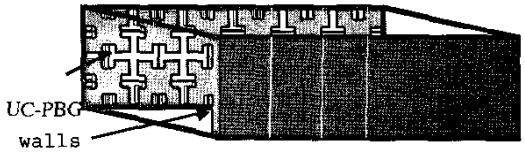

Fig. 3. UC-PBG rectangular waveguide.

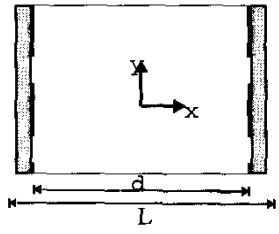

Fig. 4. Cross sectional view of the UC-PBG waveguide.

Fig. 4 shows the front view of the waveguide loaded with two UC-PBG structures located as sidewalls. The outer and inner widths are 22.86 and 21.59 mm, respectively. These UC-PBG structures were printed on a Duroid 6010 substrate with dielectric constant equal to 10.2 and dielectric thickness equal to 0.635 mm. The period of the lattice is 4.572 mm, corresponding to a resonant frequency of 10 GHz.

V. NEUROCOMPUTACIONAL TECHNIQUE

A. Introduction

Recently, it was observed a great interest in the application of artificial neural networks (ANNs) in the analysis, design, and optimization of microwave and millimeter waves circuits and devices [3]-[8].

The methodology of the neurocomputacional technique consists of the presentation to the neural network of a dataset of training examples, $\{ \boldsymbol{x}_t, f(\boldsymbol{x}_t) \}$. Then, the learning process is initialized by correcting the error between the network output, $F(w, \boldsymbol{x}_t)$ and the desired output, $f(\boldsymbol{x})$, to implement the supervised training algorithms. Finally, the validation of the neural network is accomplished by using a different dataset of examples, $\{ \boldsymbol{x}_v, f(\boldsymbol{x}_v) \}$. This includes a test of the generalization ability of the ANN that is performed by using a new set of input values.

The neural networks commonly used in applications in microwaves are: MLP, RBF, and wavelet networks. Nevertheless, in some particular microwave applications these conventional techniques do not offer good outputs.

B. Sample Function Neural Network

This new paradigm proposed in [3] is defined as Sample Function Neural Network (SFNN) and is based on the properties of the *sinc* function in signal processing theory, RBF neural network configuration, and Shanon and Littlewood-Palley wavelets. The sample activation function is shown below.

$$sample(x) = sinc(x/\pi) = sin(x)/x \qquad (1)$$

The next step was accomplished by modifying the argument of the activation function. Then, the proposed activation function was rewritten as:

$$\varphi(\boldsymbol{x},\boldsymbol{t}) = sample(\sigma^2\|\boldsymbol{x}-\boldsymbol{t}\|^2) = \frac{sen(\sigma^2\|\boldsymbol{x}-\boldsymbol{t}\|^2)}{\sigma^2\|\boldsymbol{x}-\boldsymbol{t}\|^2} \qquad (2)$$

where t accounts for translation, and σ for dilation.

The basic configuration of the SFNN model used in modeling UC-PBG microwave circuits is shown in Fig. 5.

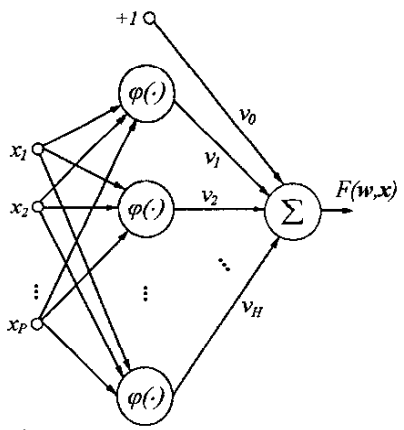

Fig. 5. Basic configuration of the SFNN neural network.

The direct computation of the SFNN neural networks is defined by the following expressions:

$$net_h = \sigma_h\|\boldsymbol{x}-\boldsymbol{t}_h\|^2 = \sigma_h(\boldsymbol{x}-\boldsymbol{t}_h)^T\cdot(\boldsymbol{x}-\boldsymbol{t}_h) \qquad (3)$$

$$y_h = \varphi(\boldsymbol{x},\boldsymbol{t}_h) = sample(net_h) \qquad (4)$$

$$F(w,x) = \sum_{h=1}^{H} v_h y_h + v_0 \qquad (5)$$

where net_h is the h^{th} internal activation potential, y_h is the h^{th} hidden neuron output , v_h is the h^{th} weight between h^{th} hidden neuron and output layer, $F(w,x)$ is the neural model output, and H is the number of hidden units.

In the supervised training process of the SFNN technique, the free parameters of the SFNN model, $\boldsymbol{w} = [\boldsymbol{V},\boldsymbol{\sigma},\boldsymbol{t}]$, are improved to diminishes the following quadratic objective function:

$$E(\boldsymbol{w},\boldsymbol{x}) = \frac{1}{2}e^2 = \frac{1}{2}[f(\boldsymbol{x}) - F(\boldsymbol{w},\boldsymbol{x})]^2 \qquad (7)$$

This was accomplished by using the gradient method:

$$\Delta\boldsymbol{w} = -\eta\nabla\boldsymbol{E} \qquad (8)$$

where η is the step-size.

VI. NUMERICAL RESULTS

In the analysis of the microstrip line on a UC-PBG the input variable is the operating frequency range from 1 to 20 GHz. The outputs of the SFNN model are: return loss, S_{11}, and insertion loss, S_{21}. The training set consisted of 100 examples, while the validation set of 37 examples, for a hidden layer with 23 neurons.

Fig. 6 shows the validation of the SFNN model for a microstrip line on a UC-PBG ground plane [6]. Note that there is an excellent agreement between the insertion loss values and the corresponding SFNN outputs, showing the accuracy of the performed neurocomputation analysis. In addition, the SFNN model outputs showed better approximation than the FDTD results.

In the analysis of the UC-PBG waveguide shown in Fig. 8, we used a basic architecture for the SFNN model, with three layers: the input layer, or the operating frequency, given in GHz, the hidden layer with 50 neurons, and the output layer, or the normalized phase velocity (v_p/c).

In the training process, 30 examples were used, corresponding to measured results presented in [4]. A learning rate of 0.1 was used and after 1000 training epochs, the final average error, SSE, was lower than $1.0\text{x}10^{-4}$.

The results for the normalized phase velocity, v_p/c, as function of frequency, are shown in Fig. 7. To validate the proposed technique an additional set of measured results was presented in Fig. 8. A good agreement was observed between this dataset and the answers of the neurocomputational technique.

C. Electric Field Distribution in the UC-PBG Waveguide

In the analysis of the electric field distribution in the UC-PBG waveguide, two input layers were assumed: the operating frequency and the position of the electric field measurement.

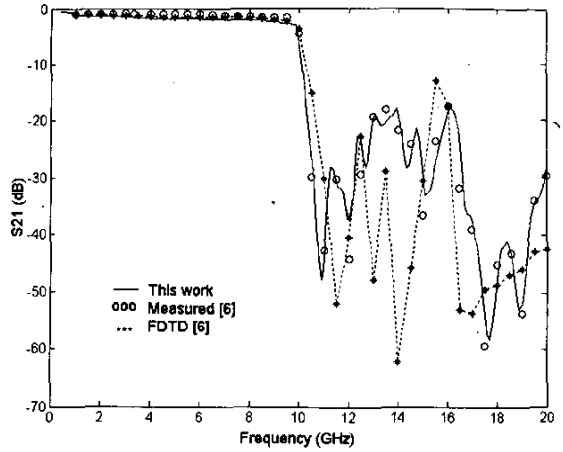

Fig. 6. Insertion loss frequency dependence for a microstrip line on a UC-PBG ground plane.

A hidden layer with 30 neurons was considered. The output layer was the electric field magnitude. A hidden layer with 30 neurons was considered and the output layer was the electric field magnitude. In the learning process, it was used a set of 100 examples, or measured results obtained in [8]. After 2000 epochs of teaching, at a learning rate of 0.01, the SFNN network got a final error (SEE) equal to 0.08×10^{-4}.

The response of the SFNN network for a passband PBG waveguide is shown in Fig. 8. The center position in the PBG waveguide is at x = 0, and the magnetic wall at x = 1.

It was observed that the interpolation results of the proposed SFNN model for four different positions in the UC-PBG waveguide show excellent agreement with a set of 30 measured values obtained from [8] and used in the validation step.

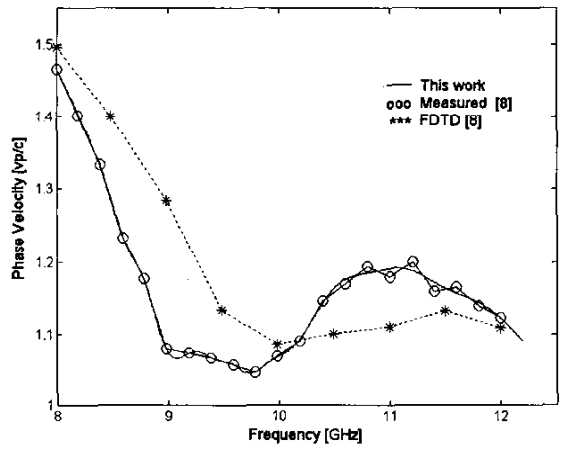

Fig. 7. Normalized phase velocity versus frequency for UC-PBG waveguide.

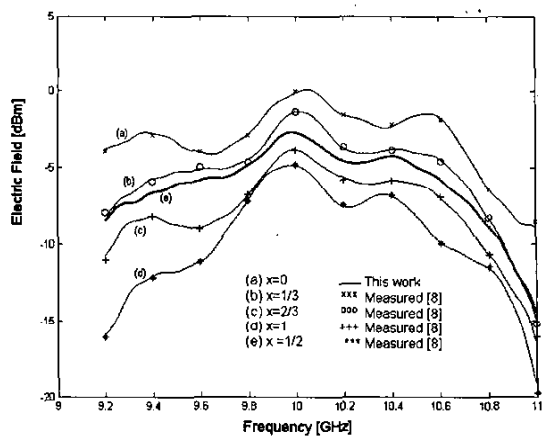

Fig. 8. Validation of the SFNN model for the UC-PBG waveguide and generalization for a new position.

VII. CONCLUSION

A new, efficient, and accurate SFNN model was used in the analysis of UC-PBG microstrip lines. It was also used to investigate the frequency dependence of the normalized phase velocity and the electric field distribution in a PBG rectangular waveguide.

The SFNN model outputs showed good agreement with the corresponding measured results available in the literature, as well as generalization ability.

REFERENCES

[1] V. Radisic, Y. Qian, R. Coccioli, and T. Itoh, "Novel 2-D Photonic Band-Gap Structures for Microstrip Lines", *IEEE Microwave Guided Wave Lett.*, vol. 8, n. 2 pp. 69-71, 1998.

[2] I. Rumsey, M. Piket-May, and P. K. Kelly, "Photonic Band-Gap Structures Used as Filters in Microstrip Circuits", *IEEE Microwave Guided Wave Lett.*, vol. 8, pp. 336-338, 1998.

[3] E. N. R. Q. Fernandes, P. H. F. Silva, M. A. B. Melo, and A. G. d'Assunção, "A New Neural Network Model for Accurate Analysis of Microstrip Filters on PBG Structure", *European Microwave Conf. Dig.*, Milan, Italy, 2002.

[4] J. D. Joannopoulus, R. Meade, and E. J. Winn, *Photonic Crystal, Molding the Flow of Light*, Princeton University Press, NJ, 1995.

[5] Q. J. Zhang and K. C. Gupta, *Neural Networks for RF and Microwave Design*, Artech House, Boston, 2000.

[6] F. Yang, K. Ma, Y. Quian, and T. Itoh, "A Uniplanar Compact Photonic Band-Gap (UC-PBG) Structure and its Applications for Microwave Circuits", *IEEE Trans. Microwave Theory Tech.*, vol. 47, pp. 1509-1514, 1999.

[7] C. Christodoulou and M. Georgiopoulos, *Applications of Neural Networks in Electromagnetics*, Artech House, 2001.

[8] F. Yang, K. Ma, Y. Quian, and T. Itoh, "A Novel TEM Waveguide Using Uniplanar Compact Photonic-Bandgap (UC-PBG) Structure", *IEEE Trans. Microwave Theory Tech.*, vol. 47, n. 11, pp. 2092-2098, 1999.